Modern Physics Letters B
Vol. 28, No. 23 (2014) 1450188 (8 pages)

DOI: 10.1142/S0217984914501887

A band-pass plasmonic filter with dual-square ring resonator

Gaoyan Duan*, Peilin Lang†, Lulu Wang, Li Yu and Jinghua Xiao
School of Science, Beijing University of Posts and Telecommunications,
P. O. Box 123, Beijing 100876, China
**gaoyanduan@bupt.edu.cn*
†*lang.peilin@gmail.com*

Received 16 May 2014
Revised 20 July 2014
Accepted 13 August 2014
Published 10 September 2014

In this paper, we show the simulation of a plasmonic band-pass filter which consists of two surface plasmon polaritons (SPPs) waveguides and a resonator in metal–insulator–metal (MIM) structure. The resonator is formed by two square rings and a patch between them. The patch is a tiny rectangle cavity in order to transfer the SPPs from one ring to the other. The finite element method (FEM) method is employed in simulation. The results show that the dual-ring resonator performs better than a single ring does. The 3 dB bandwidth near the peak wavelength $\lambda = 1054$ nm is merely 31.7 nm. The resonant wavelength can be shifted by changing the side length of the square ring. This narrow band-pass filter is easy to fabricate and has potential applications in future integrated optical circuits.

Keywords: Surface plasmon polaritons; MIM waveguide; plasmonic filter.

1. Introduction

Surface plasmon polaritons (SPPs) are electromagnetic waves propagating along a metal–dielectric interface with an exponentially decaying field in both sides.[1,2] Because the SPPs can carry energy and information to overcome the diffraction limit of light, it has been considered as one of the most potential ways of realization of highly integrated optical circuits in future nanophotonic systems. The insulator–metal–insulator (IMI) structure and metal–insulator–metal (MIM) waveguide structure[3–23] have been proposed to confine and channel the light because they have two metal–dielectric interfaces close to each other and can guide SPPs in a low-loss symmetric couple mode. Due to the good properties on strong field confinement, the MIM structures have been applied in a lot of SPP optical elements, such as modulators,[5] filters,[6,7] optical attenuators,[8] switches,[9] grating,[17] and so on.

Filter is a basic element in SPP waveguide. Yun *et al* proposed an SPP band-pass filter based on a rectangle ring resonator.[10] Peng *et al.* used the square-ring

resonator to form a band-stop filter.[11] Resonator of slot cavity and other shapes have been proposed.[12,18–22] Filter based on a double-ring resonator has been reported in microwave and optical waveguide.[14,15] However, the SPP waveguide has also disadvantages such as large loss and tiny size. The results from microwave cannot be simply applied in the field of SPPs. Chen *et al.* studied the properties of an SPP filter with a double-ring resonator.[23] To our knowledge, there has been no report on SPP resonator of two square-rings in MIM structures.

In this paper, we propose a two-dimensional (2D) MIM nanoscale structure composed of waveguides and a resonator of two square rings. Finite element method (FEM) is employed to study the transmission characteristics of the SPP filter. The results show that the 3 dB bandwidth is very narrow. By changing the size of the resonator, the resonant wavelength of the high performance band-pass filter can be adjusted.

2. Structures and Method

Figure 1(a) shows the structure of proposed band-pass filter based on square-ring geometry which consists of an input waveguide, two square rings, a patch between the two square rings, and an output waveguide. The patch is a tiny rectangle hole coupled with the two rings. For the sake of comparison, a single square-ring resonator filter is shown in Fig. 1(b), which is proposed by Refs. 10 and 11. The white and gray parts in Fig. 1 represent air and silver, respectively.

In our band-pass filter, as shown in Fig. 1(a), the waveguides, the square rings and the patch are coupled one by one with a gap width g. The widths of the waveguides and of the square rings are set as t and d, respectively. L is the inner

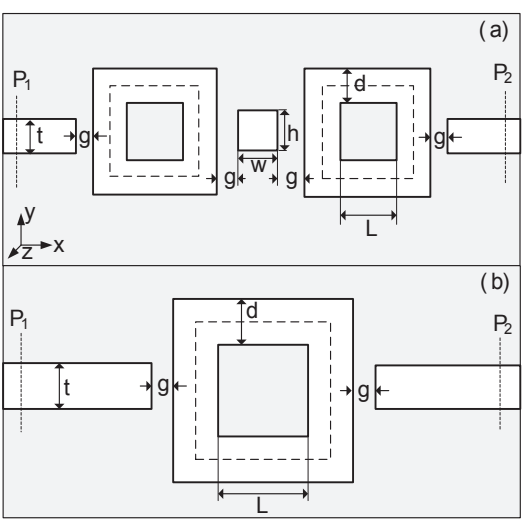

Fig. 1. The schematics of (a) double-square ring filter and (b) the single-ring filter based on SPPs.

side length of the square ring. We define an average perimeter of the square $L_a = 4(L + d)$, as illustrated by the dashed line in Fig. 1. Parameters w and h are respectively the width and height of the patch.

The waveguide width and the square ring width are set as $t = d = 50$ nm. For MIM waveguides, only the transverse magnetic (TM) modes can be supported. The dispersion equation of SPPs in the MIM structure can be written as follows:[15,16]

$$\tanh\left(\frac{k_1 d}{2}\right) = -\frac{k_2 \varepsilon_1}{k_1 \varepsilon_2}\,, \tag{1}$$

where ε_1 and ε_2 denote the dielectric constants of the air and the silver layer, respectively. The wave vectors k_1 and k_2 can be denoted by $k_1 = \sqrt{\beta^2 - \varepsilon_1 k_0^2}$ and $k_2 = \sqrt{\beta^2 - \varepsilon_2 k_0^2}$. β is the propagation constant of the MIM waveguide and k_0 means the free-space wave vector. We assume the permittivity in the air is 1.0. The permittivity in silver is frequency dependent, and the Drude model is employed to characterize the dielectric constant[17,18]

$$\varepsilon_2(\omega) = \varepsilon_\infty - \frac{\omega_n^2}{\omega^2 - i\omega\Gamma_0}\,, \tag{2}$$

where $\varepsilon_\infty = 3.7$ is the relative permittivity at infinite frequency, $\omega_n = 13{,}800$ THz is the bulk plasma frequency and $\Gamma_0 = 27.3$ THz is the damping constant.

FEM is employed to simulate the transmission characteristics of the SPP filters. We use a plane wave source to excite the SPPs. The SPPs excited by the light propagate through the left waveguide, and enter the left square ring, then go on through the patch between two square rings, travel in the right square ring, and at last transmit to the right waveguide. Two power monitors are used to detect the input and output energy currents P_1 and P_2, as shown by the straight dash line in Figs. 1(a) and 1(b). Because the reflected wave is much weaker than the input wave, we ignored the reflection of SPP. So the transmittance is defined as $T = P_2/P_1$. The scattering boundary conditions are used to avoid the reflection at the calculation boundary.

3. Results and Discussion

Figure 2 shows the transmission spectrum of the band-pass plasmonic filter. The solid and dash lines correspond to the double-square ring and single-square ring structures, respectively.

We set the parameters of the double-square ring structure as $t = d = 50$ nm, $g = 20$ nm, and $L = 150$ nm. The structure of the single ring filter is ever used in Refs. 10–12, and the values are the same with the double-square ring structure. In addition, the width and height of the patch in the double-square ring structure are set as 20 nm and 50 nm, respectively. From Fig. 2, the double-ring band-pass filter has two transmission peaks corresponding to the wavelength $\lambda = 535$ nm and $\lambda = 1054$ nm. The peak value reaches 0.5763 at $\lambda = 535$ nm. While the low transmission values at the stop-band never reach over 10^{-5}. The minimum is merely

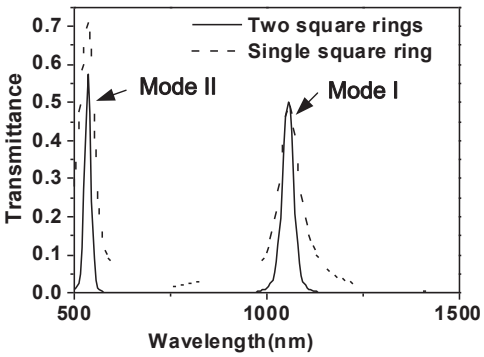

Fig. 2. The transmission spectrum of the band-pass plasmonic filter.

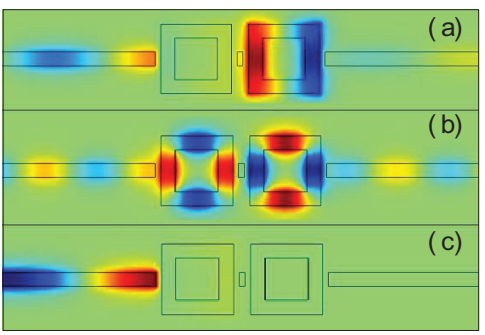

Fig. 3. (Color online) The contour profiles of field Hz of proposed band-pass filter at wavelengths (a) $\lambda = 1054$ nm, (b) $\lambda = 535$ nm and (c) $\lambda = 1500$ nm.

3.2×10^{-7}. For the valley value is almost 0, the peak-to-valley ratio of this mode is 1.8×10^6, and the 3 dB bandwidth near $\lambda = 1054$ nm is about 31.7 nm. The small 3 dB bandwidth indicates that the edges of the pass band are very sharp. In contrast, for the single-square ring filter, whose resonant modes are at nearly the same wavelengths, the maximum peak-to-valley ratio is about 1.5×10^3. And the 3 dB bandwidth is 39.3 nm. Those results are worse than that of the double-square ring resonator. Moreover, the rising edge and trailing edge of two peaks in double-square ring structure vary more quickly and the valley is more flat. Figure 3 shows the contour profiles of field Hz of two modes in the double-ring structure. Modes I and II, whose peak wavelengths are 1054 nm and 535 nm, correspond to Figs. 3(a) and 3(b), respectively. It is clear that only the light with a resonant wavelength can be easily transmitted through the filter. In contrast, the field distribution at the non-resonant mode is shown in Fig. 3(c).

The role of the patch is shown in Fig. 4. As shown in the inset of Fig. 4(a), we set the width of the patch as zero, so the patch is removed. It is clear that each resonant peak splits. The second peak in each mode comes from an orthogonal mode in which

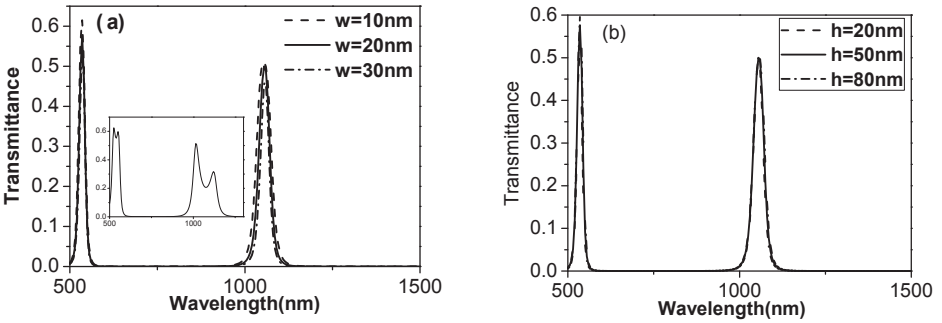

Fig. 4. Transmittance spectrum of band-pass filter with respect to only altering the width (a) or height (b) of the patch.

the field distribution patterns of the two resonant rings are orthogonal to each other. The two rings in a dual-ring resonator without a patch are directly coupled each other and must be regarded as a whole resonator. This whole resonator contains complicated modes which widen the 3 dB bandwidth. While the patch translates the direct coupling into an indirect one. The two rings can be regarded as two separated resonators and each one only contains simple resonant modes. Thus, the patch can block the orthogonal mode and makes the 3 dB bandwidth thinner. And this is the reason why the peaks for single and two ring cases coincide shown in Fig. 2. Due to the role of the patch, it is obviously that the dual-square-ring resonator is not a simple repeat of a dual-circle-ring resonator proposed by Ref. 24. The transmission spectra of SPPs for different width w and height h are shown in Figs. 4(a) and 4(b), while the other parameters keep unchanged. From the figure, both the width and the height of the patch have little effect on the transmittance. What is more, we also find that the transmittance of SPPs is nearly constant when the position along y-direction of the patch changes.

The transmission spectra of SPPs for different side length L of two square rings with the fixed width d are shown in Fig. 5. The dash, solid, dot and dash dot lines correspond to the side length L equals to 140, 150, 160 and 170 nm, respectively. It can be seen that, when the side length changes from 140 nm to 170 nm, the peak of the transmission spectrum exhibits a redshift obviously. The mode I shifts larger than the mode II, and transmittance peak of the modes decreases monotonically. But 3 dB bandwidth of each mode varies little. This result is in accordance with the fact that increasing square side length means adding the total cavity length of two square rings. Of course the resonant wavelength will increase. On the other hand, increasing the cavity length means to add transmittance loss. So the transmittance intensity will decrease. If the resonator contains three coupled rings or more, the transmittance intensity will be too small. It is clear that the band-pass filter can be tuned by adjusting the dimensions of the two square rings.

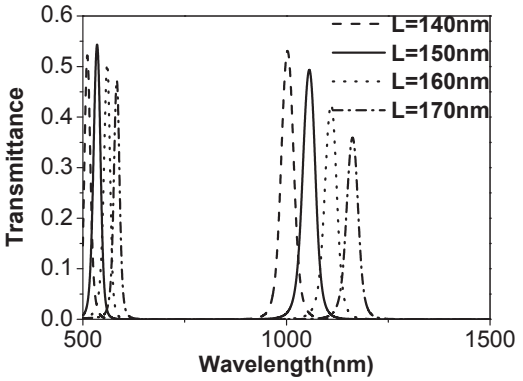

Fig. 5. Transmittance spectrum of band-pass filter with different square side length from 140 nm to 170 nm.

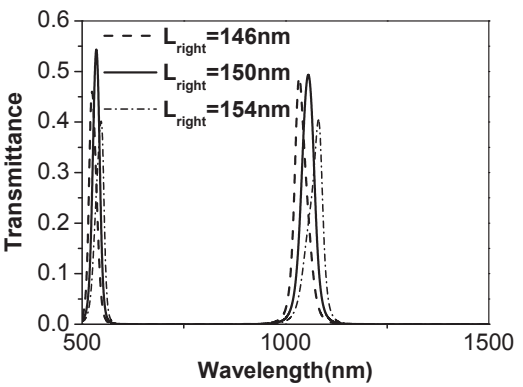

Fig. 6. Transmittance spectra of band-pass filter with respect to only altering side length of the right square ring.

Our preceding work shows that a filter with an asymmetric double-ring resonator may lead a better performance.[24] Thus, we study the effect of two square rings with different sizes. Figure 6 shows transmission spectra with different inner side length L_{right} of the right square ring while keeping other dimensions constant, i.e. d and g are kept constant. And the inner side length of the left square ring is set as $L_{\text{left}} = 150$ nm. From the figure, a redshift is observed in the resonance wavelengths with an increasing right inner side length L_{right}. These results are in complete accordance with the fact that increasing the side length of the right square ring means to increase the total cavity length of the structure. And it is obvious that the transmittance wavelength will increase. The 3 dB bandwidth still keeps changeless. Unlike the filter in Ref. 24, the transmittance intensity is the largest when two square rings have the same size. When two square rings are same, perfectly matched conditions are satisfied. Thus, the transmittance intensity is obviously the strongest.

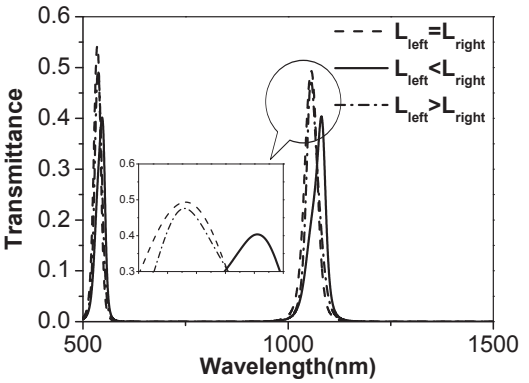

Fig. 7. Transmittance spectrum of band-pass filter with respect to only altering side length of two square rings, $L_{\text{left}} = L_{\text{right}} = 150$ nm, $L_{\text{left}} = 150$ nm $< L_{\text{right}} = 154$ nm, $L_{\text{left}} = 154$ nm $> L_{\text{right}} = 150$ nm, keeping the others constant.

We also find the right square ring plays an important role in deciding the center wavelength of each mode. As shown in Fig. 7, the dash, solid and dash dot lines correspond to three arrangements respectively: $L_{\text{left}} = L_{\text{right}} = 150$ nm, $L_{\text{left}} = 150$ nm and $L_{\text{right}} = 154$ nm and $L_{\text{left}} = 154$ nm and $L_{\text{right}} = 150$ nm. The enlarged view of the peak of the mode I is shown in the inset of Fig. 7. It is obvious that the peaks are nearly at the same center wavelength when $L_{\text{right}} = 150$ nm. While with $L_{\text{right}} = 154$ nm, the peak shift to a long wavelength obviously. So we obtain the conclusion that the center wavelength of each mode is mainly decided by the right square ring.

This effect comes from the influence of the patch. Due to the patch, the dual-ring resonator can be regarded as two separated single ring resonators coupled indirectly to each other by the patch. Thus, the wave which can be coupled into the right ring must match the resonant condition. Because the size of the right ring is different from the left one, the wave at the left resonant wavelength is mostly reflected at the patch by the right ring, while the wave at the right resonant wavelength can be coupled into the right ring completely. This is the reason why the right ring plays an important role to decide the center wavelength of each transmittance peak. In contract, the two rings in a dual-ring resonator without the patch are coupled each other directly and play a similar role on the peak position.

4. Conclusion

In conclusion, we have presented a novel nanoscale waveguide structure coupled with a resonator of double square rings to act as a band-pass filter. The transmission spectra of the filter are calculated by the FEM method. The results show that the two-square-ring band-pass filter has better sensitivity on the wavelength than the one with a single ring. With increasing the square side length, the characteristic wavelengths of the band-pass filter have a red shift. That means we can easily control

the characteristic wavelength by changing the square side length. And moreover, we find that the center wavelength of each mode is mainly decided by the right square ring. This band-pass filter is easy to realize, and has potential applications on optical integrated circuits.

Acknowledgments

This work was supported by the National Basic Research Program of China under Project (2010CB923202) and the Natural Science Foundation of Shandong Province (ZR2012FL21).

References

1. P. Berini and I. De Leon, *Nat. Photon.* **6** (2011) 16.
2. H. Raether, *Surface Plasmons on Smooth and Rough Surfaces and on Gratings* (Springer-Verlag, Berlin/New York, 1988).
3. P. Berini, *Phys. Rev. B* **61** (2000) 10484.
4. J. Park, H. Kim and B. Lee, *Opt. Express* **16** (2008) 413.
5. T. Nikolajsen, K. Leosson and S. I. Bozhevolnyi, *Opt. Commun.* **244** (2005) 455.
6. X. Zhai *et al.*, *J. Nanomaterials* **2013** (2013) 484207, http://dx.doi.org/10.1155/2013/484207.
7. D. Xiang and W.-J. Li, *J. Mod. Opt.* **61** (2014) 222.
8. G. Gagnon, N. Lahoud, G. A. Mattiussi and P. Berini, *J. Lightwave Technol.* **24** (2006) 4391.
9. T. Nikolajsen, K. Leosson and S. I. Bozhevolnyi, *Appl. Phys. Lett.* **85** (2004) 5833.
10. B.-F. Yun, G.-H. Hu and Y.-P. Cui, *J. Phys. D: Appl. Phys.* **43** (2010) 385102.
11. X. Peng, H.-J. Li, C. Wu, G.-T. Cao and Z.-M. Liu, *Opt. Commun.* **294** (2013) 368.
12. B.-F. Yun, G.-H. Hu and Y.-P. Cui, *Opt. Commun.* **305** (2013) 17.
13. J.-L. Liu, G.-Y. Fang, H.-F. Zhao, Y. Zhang and S.-T. Liu, *J. Phys. D: Appl. Phys.* **43** (2010) 055103.
14. I. Chremmos and N. Uzunoglu, *IEEE Photon. Technol. Lett.* **17** (2005) 2110.
15. A. E. Cetin and O. E. Mustecaplioglu, *Phys. Rev. A* **81** (2010) 043812.
16. H. Lu, X. Liu, D. Mao, Y. Gong and G. Wang, *J. Opt. Soc. Am. B* **28** (2011) 1616.
17. Z. H. Han, E. Forsberg and S. He, *IEEE Photon. Technol. Lett.* **19** (2007) 91.
18. Y. Cui and C. Zeng, *Appl. Opt.* **51** (2012) 7482.
19. I. Zand, A. Mahigir, T. Pakizeh and M. S. Abrishamian, *Opt. Express* **20** (2012) 7516.
20. P. Chen, R. Liang, Q. Huang and Y. Xu, *Opt. Commun.* **284** (2011) 4795.
21. B. Yun, G. Hu and Y. Cui, *Plasmonics* **8** (2013) 267.
22. V. F. Nezhad, S. Abaslou and M. S. Abrishamian, *J. Opt.* **15** (2013) 055007.
23. X. Che, P. Lang, G. Li, R. Zhang and T. Zhong, *J. Mod. Opt.* **60** (2013) 1911.
24. C. Xi *et al.*, *J. Mod. Opt.* (2014), http://www.tandfonline.com/doi/full/10.1080/09500340.2014.909956.